Available online at www.sciencedirect.com
SCIENCE DIRECT
Polymer 46 (2005) 7823–7833
polymer
www.elsevier.com/locate/polymer

Synthesis and characterization of poly(ester amide)s containing crystallizable amide segments

P.A.M. Lips[a], R. Broos[b], M.J.M. van Heeringen[b], P.J. Dijkstra[a], J. Feijen[a,*]

[a]*Department of Polymer Chemistry and Biomaterials, Faculty of Science and Technology, Institute for Biomedical Technology (BMTI), University of Twente, P.O. Box 217, 7500 AE Enschede, The Netherlands*
[b]*Core R&D, Dow Benelux NV, P.O. Box 48, 4530 AA Terneuzen, The Netherlands*

Received 21 March 2005; received in revised form 30 June 2005; accepted 5 July 2005

Abstract

High molecular weight segmented poly(ester amide)s were prepared by melt polycondensation of 1,4-butanediol, dimethyl adipate and a preformed bisamide-diol based on 1,4-diaminobutane and ε-caprolactone. By varying the ratio of the bisamide-diol and 1,4-butanediol, a series of polymers was obtained with a hard segment content between 10 and 85 mol%. FT-IR and WAXD analysis revealed that the poly(ester amide)s crystallize in an α-type phase similar to the α-phase of even–even nylons. These polymers all have a micro-phase separated structure with an amide-rich hard phase and an ester-rich flexible soft phase. The polymers have a low and a high melt transition, corresponding with the melting of crystals comprising single ester amide sequences and two or more ester amide sequences, respectively. The low melt transition is between 58 and 70 °C and is independent of polymer composition. By increasing the hard segment content from 10 to 85 mol% the high melt transition increased from 83 to 140 °C while the glass transition temperature increased from −45 to −5 °C. Likewise, the elastic modulus increased from 70 to 524 MPa, the stress at break increased from 8 to 28 MPa while the strain at break decreased from 820 to 370%. Thermal and mechanical properties can thus be tuned for specific applications by varying the hard segment content in these segmented polymers.

Keywords: Poly(ester amide); Crystallization; Structure–property relations

1. Introduction

Aliphatic polyesters, such as poly(ε-caprolactone) and poly(butylene adipate) are biodegradable, but lack the physical and mechanical properties necessary for a broad range of applications. Synthetic aliphatic polyamides are generally not biodegradable but have favourable crystallization properties, good solvent and heat stability and high moduli and tensile strength. Combination of the characteristics of both groups of polymers may be achieved by the synthesis of aliphatic poly(ester amide)s in which amide groups are randomly distributed in the polymer chain [1–13] or in which well-defined amide group containing blocks or segments are incorporated in the polymer [11,14–19].

Segmented poly(ester-amide)s consisting of rigid amide segments and amorphous flexible ester segments are thermoplastic elastomers [20]. These polymers have a micro-phase separated structure with an amide-rich hard phase and an ester-rich soft phase. The amide-rich phase usually contains crystalline lamellae and acts as a thermo-reversible physical crosslinker for the amorphous phase. The soft phase has a sub-ambient glass transition temperature (T_g) and contributes to the flexibility and extensibility of the polymer. Heating above the melting temperature of the hard domains usually results in phase mixing of hard and soft segments. Without the reinforcing tie points, the polymer will flow as a thermoplastic material and can easily be melt processed. Upon cooling, the hard and soft segments become incompatible, which leads to phase separation into micro-domains and crystallization and thus to reformation of the physical crosslinks. Previous research revealed that an effective way to improve phase separation is using short, symmetrical and uniform amide blocks [21–24].

* Corresponding author. Tel.: +31 534 892 968.
E-mail address: j.feijen@tnw.utwente.nl (J. Feijen).

0032-3861/$ - see front matter © 2005 Published by Elsevier Ltd.
doi:10.1016/j.polymer.2005.07.013

Aliphatic segmented poly(ester amide)s containing uniform hard blocks have received limited attention. Segmented poly(ester-amide)s prepared from preformed bisamide-diols and oligoesters were synthesized by Bera et al. [18,19]. The bisamide-diol prepared from 1,6-diaminohexane and γ-butyrolactone, was first reacted with adipic acid to form a hard alternating poly(ester amide) oligomer. The oligoester (soft block) was prepared from 1,2-ethanediol and dimethyl adipate. A series of high molecular weight polymers was obtained by reacting various ratios of hard and soft oligomers. By increasing the hard oligomer content from 20 to 80 mol% the modulus increased from 70 to 600 MPa and the yield stress increased from 0.04 to 15 MPa. All polymers have two glass transition temperatures (−40 to −50 and 40 to 50 °C) and one melting temperature at ∼200 °C, indicating the presence of two separate amorphous domains and a crystalline phase. Hydrogen bonding, studied with temperature dependent IR, showed that amide–amide and ester–amide H-bonds were formed in all polymers [25,26]. It was concluded that the ester–amide H-bonds are stable up to 210 °C whereas the amide–amide H-bonds disappear at 170 °C.

Stapert et al. prepared segmented block poly(ester amide)s by condensation of preformed bisamide-diols or bisamide-diesters, 1,4-butanediol and dimethyl adipate in the melt [14,15,27]. The uniform amide blocks were randomly distributed in the polymer chain and during the polycondensation reaction no or little ester–amide interchange occurred between segments of the polymer chain. These polymers show an endothermic transition between 50 and 70 °C followed by a melting temperature, which increased from 80 to 140 °C by increasing the hard segment content from 10 to 100 mol%. The higher transition corresponds to the melting of a crystalline phase consisting of crystals composed of two or more subsequent ester amide (EA) sequences. The first melt transition, which is independent of the amide content of the polymer, is attributed to melting of crystals comprising single EA sequences. This crystalline phase is meta stable with respect to the higher melting crystalline phase [28]. The glass transition temperature increases with increasing hard segment content, indicating a homogenous amorphous phase.

The ratio of hard to soft segments, affects the properties of segmented poly(ester amide)s as the polymer changes from a more soft polyester to a hard polyamide. In this paper, the influence of the amount of hard segment in segmented poly(ester amide)s based on a *N*,*N*′-1,4-butanediyl-bis[6-hydroxy-hexanamide], dimethyl adipate and 1,4-butanediol, on the thermal, physical and mechanical properties is described.

2. Experimental

2.1. Materials

1,4-Butanediol, dimethyl adipate (synthetic grade) chloroform-d_1 and the catalyst tetrabutylorthotitanoate ($Ti(OBu)_4$) were purchased from Merck, Germany. The anti-oxidant Irganox 1330 was kindly provided by Ciba Geigi, Switzerland. Trifluoroacetic acid-d_1 was obtained from Aldrich, The Netherlands. All other solvents were obtained from Biosolve, The Netherlands. The synthesis of *N*,*N*′-1,4-butanediyl-bis[6-hydroxy-hexanamide] is described previously (T_m = 144 °C) [29].

2.2. Poly(ester amide) synthesis

The synthesis of the copolymer based on *N*,*N*′-1,4-butanediyl-bis[6-hydroxy-hexanamide], 1,4-butanediol and dimethyl adipate (DMA) was carried out as previously described [14]. Small adjustments were implemented to scale up the polymerization to ∼100 g.

The molar ratio of hard (x) and soft (y) segments in the poly(ester amide) is varied by changing the ratio of *N*,*N*′-1,4-butanediyl-bis[6-hydroxy-hexanamide] and 1,4-butanediol.

A typical procedure for the preparation of PEA 72/28 containing 28 mol% of hard segment is described hereafter in detail. Dimethyl adipate (70.00 g, 0.402 mol), *N*,*N*′-1,4-butanediyl-bis[6-hydroxy-hexanamide] (31.79 g, 0.101 mol) and a twofold excess of 1,4-butanediol (54.07 g, 0.602 mol) were placed in a polymerization tube. To the mixture ∼1 ml of a stock solution (0.15 g ml^{-1}) of $Ti(OBu)_4$ in toluene and Irganox 1330 (1.55 g = 1.0 wt% of total mass) were added. The amount of catalyst used was always 2 mg $Ti(OBu)_4$/g DMA. The mixture was stirred for 15 min at room temperature under an argon atmosphere. The pressure was reduced to 500 mbar and subsequently the mixture was slowly heated to 180 °C over a period of 3 h. The methanol distilled off during this period and was collected in a trap, cooled with ice water. Subsequently, the pressure was slowly decreased to ∼100 mbar. The reaction vessel was cooled to room temperature under vacuum and left to stand over night. An additional 0.14 g of catalyst was added. The reaction mixture was heated to 180 °C under reduced pressure (500 mbar). In the next 2 h, the pressure was decreased to 5 mbar. The temperature was increased to 190 °C and the pressure was very slowly decreased to 0.15 mbar. The trap was cooled with liquid nitrogen, which reduced the pressure to 0.1 mbar. The excess of 1,4-butanediol was distilled off during the next 5 h. The final pressure was 0.04 mbar. The reaction mixture was then cooled to room temperature under vacuum. The polymer was dissolved in 100 ml of chloroform at 55 °C for 2 h and subsequently precipitated in 4 l of diethyl ether. The polymer was filtered, washed with cold diethyl ether and dried overnight at room temperature at reduced pressure.

The polymers PBA, PEA 90/10, PEA 72/28, PEA 44/56, PEA 22/78 and PEA 15/85 with a hard segment content x of 0, 10, 28, 56, 78 and 85 mol%, respectively, were prepared according to the method described above.

2.3. Methods

2.3.1. NMR

^{1}H (300 MHz) and ^{13}C (75.26 MHz) NMR spectra were recorded on a Varian Inova nuclear magnetic resonance spectrometer using chloroform-d_1 or trifluoracetic acid-d_1 as a solvent.

2.3.2. Viscometry

Intrinsic viscosities [η] were determined by a single point measurement using a capillary Ubbelohde type 0C at 25 °C and a polymer solution with a concentration of 0.1 g dl^{-1} in chloroform–methanol (1:1 vol/vol) [30,31]. The following empirical equation was applied:

$$[\eta] = \frac{\sqrt{2}}{c}\sqrt{\eta_{spec} - \ln \eta_{rel}} \quad (1)$$

where $\eta_{spec} = \eta_{rel} - 1$ and c is the polymer concentration in g dl^{-1}.

The intrinsic viscosity of PEA 72/28 was also determined by extrapolation of η_{rel} and η_{inh} to $c = 0$.

2.3.3. FT-IR

Fourier transform infrared spectra were recorded with a Biorad FTS 175 spectrometer utilizing a wide band MCT detector at 4 cm^{-1} spectral resolution. Thin polymer films were placed between sodium chloride windows and transferred to a heatable infrared cell from Specac Inc. The sample was heated to 190 °C at 45 °C min^{-1}, kept for 10 min at 190 °C, cooled to 30 °C with an average rate of 5 °C min^{-1}. Subsequently, data points were collected between 4000 and 550 cm^{-1}.

Temperature dependent FT-IR spectra of poly(butylene adipate) (PBA) were performed on melt-crystallized materials. The polymer film was first heated to 100 °C (45 °C min^{-1}), kept for 10 min at 100 °C and cooled to 30 °C with an average rate of 5 °C min^{-1}. The sample was then heated to 100 °C in steps of 10 °C at a heating rate of 45 °C min^{-1}. After each step the temperature was kept constant for 5 min before data collection.

The crystallinity w_c (in mol%) of the poly(ester amide)s was calculated according to:

$$w_c = \left(\frac{b_1}{b_1 + b_2 + b_3}\right)x \quad (2)$$

with b_1 the band area of the amide I band at 1634 cm^{-1} (H-bonded, ordered, crystalline domains), b_2 the band area of the amide I band at ~1651 cm^{-1} (H-bonded disordered, amorphous domains), b_3 the band area of the amide I band at ~1673 cm^{-1} (non-H-bonded, amorphous domains) and x the hard segment content in mol%. Curve fitting was used to resolve the selected IR-band areas.

2.3.4. WAXD

Wide angle X-ray diffraction spectra were recorded using a Philips X'Pert-MPD diffractometer in Bragg–Brentano geometry, with a Θ compensating divergence slit (10.0 mm). The polymer film (15×10×1 mm) was mounted on a Pt filament in an Anton Paar HTK-16 temperature chamber. A Cu-anode was used, together with a curved graphite monochromator, giving Cu Kα_1 radiation of 1.5406 Å. Prior to measurement the chamber was flushed with nitrogen.

The sample was heated to 190 °C, annealed for 10 min and subsequently cooled at 20 °C min^{-1} to 30 °C. Data points were collected in the range of 2Θ is 4–90°.

The peak position at angles of 2θ correspond to interplanar d-spacings according to Bragg's law:

$$d = \frac{n\lambda}{2\sin\theta} \quad (3)$$

with n is an integer and λ is the applied wavelength (1.5406 Å).

2.3.5. TGA

Thermal gravimetric analysis was carried out with 5–10 mg samples under a nitrogen atmosphere in the 50–700 °C range at a heating rate of 10 °C min^{-1}, using a Perkin–Elmer thermal gravimetric analyser TGA-7.

2.3.6. DSC

Thermal analysis of the polymers was carried out using a Perkin–Elmer DSC-7 differential scanning calorimeter equipped with a PE7700 computer and TAS-7 software. Calibration was performed with pure indium. Measurements were performed on isolated precipitated polymers. Samples (5–10 mg) were heated from 25 to 180 °C at a rate of 20 °C min^{-1}, annealed for 5 min, cooled to −80 °C at a rate of 20 °C min^{-1}, and subsequently heated from −80 to 180 °C at a rate of 20 °C min^{-1}. Melting (T_m) and crystallization (T_c) temperatures were obtained from the peak maxima, melt (ΔH_m) and crystallization (ΔH_c) enthalpies were determined from the area under the curve and the glass transition temperature (T_g) was taken at the inflection point. The data presented are from the second heating step, unless stated otherwise.

2.3.7. Processing

Polymer bars were prepared both by compression moulding and injection moulding. Compression moulded bars (75×4×2 mm) were prepared with a hot press (THB 008, Fontijne Holland BV, The Netherlands). Polymers were heated for 6–8 min at 20 °C above their T_m as measured by DSC, pressed for 3 min at 300 kN, and cooled in approximately 5 min under pressure to room temperature. Injection moulded bars (70×9×2 mm) were prepared with an Arburg-H manual injection moulding machine. The barrel was set to 40 °C above the T_m of the polymer as determined by DSC.

2.3.8. DMA

Differential mechanical analysis was performed with a Myrenne ATM3 torsion pendulum at a frequency of approximately 1 Hz. The storage modulus (G') and the loss modulus (G'') were measured as a function of temperature. Samples (75×4×2 mm) were first cooled to −100 °C and then heated at a rate of 1 °C min^{-1}. The temperature at which the loss modulus reached a maximum was taken as the T_g. The flow temperature (T_{flow}) was defined as the temperature at which the storage modulus reached 1 MPa.

2.3.9. Tensile tests

Tensile tests were conducted with compression moulded and injection moulded bars, cut to dumbbells (ISO 37). A Zwick Z020 universal machine equipped with a 500 N load cell and extensometers was used to measure the stress as a function of strain at a strain rate of 500 mm min^{-1} and a preload of 3 N. Measurements were performed on at least six different polymer bars.

2.3.10. Compression set

Polymer samples (10×10×2 mm) cut from injection moulded bars were placed between two metal plates at 25 °C (ASTM 395 B standard) and compressed to 75% of their original thickness for 24 h. The sample thickness was determined half an hour after the load was released. The measurements were performed in triplo. The compression set (CS) is calculated according to:

$$\mathrm{CS} = \frac{d_0 - d_2}{d_0 - d_1} \times 100\% \quad (4)$$

where d_0, d_1, and d_2 are the sample thicknesses before, during, and after compression, respectively.

2.3.11. Water uptake

The polymer water absorption was determined by placing polymer bars (75×4×2 mm) in a dessicator at room temperature at 100% relative humidity (RH) for 28 days. Samples (10×10×2 mm) were also immersed in demineralised water at 37 °C for 28 days. Compression moulded samples were predried at 30 °C under reduced pressure for at least 2 days. The water absorption (wt %) is calculated from:

$$\mathrm{wt\%} = \frac{w_0 - w}{w_0} \times 100\% \quad (5)$$

where w_0 and w are the sample weights before and after treatment, respectively.

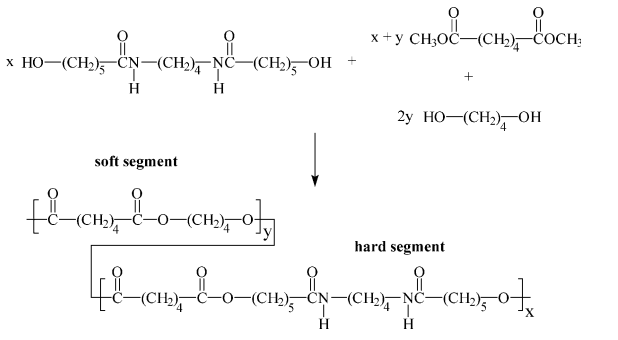

Fig. 1. Reaction scheme for the synthesis of a poly(ester amide) based on a bisamide-diol, 1,4-butanediol and dimethyl adipate.

3. Results and discussion

3.1. Characterization

Segmented poly(ester amide)s were prepared by copolymerisation of a bisamide-diol, dimethyl adipate and 1,4-butanediol in the melt (Fig. 1). The trans-esterification was performed at 180 °C at atmospheric pressure under argon for 2 h. The polycondensation started by increasing the temperature to 190 °C and reducing the pressure to ~0.1 mbar with distillation of 1,4-butanediol. The molar ratio of hard (x) and soft (y) segment of the poly(ester amide) was varied by changing the ratio of bisamide-diol to 1,4-butanediol in the monomer feed. A series of poly(ester amide)s PEA 90/10, PEA 72/28, PEA 44/56, PEA 22/78 and PEA 15/85 with a hard segment content x of 10, 28, 56, 78 and 85 mol%, respectively, were prepared in this way. The homopolymer poly(butylene adipate) (PBA) was added to the series.

Previously it has been shown that the symmetrical and uniform structure of the hard bisamide segments was retained in the polymer [14,27]. Less than 5 mol% of the symmetrical amide segments is lost due to alcoholysis of the amide bonds during the first hours of the reaction.

The composition of the poly(ester amide)s, determined by ^{1}H NMR, in almost all cases deviates slightly from the intended composition (Table 1). The deviation is becoming more pronounced at higher hard segment content. This deviation is caused by distillation of a small amount of dimethyl adipate during the polymerization, which disturbs the stoichiometry. Assuming that the polymer chains have hydroxyl end groups, ^{1}H NMR was also used to estimate the molecular weights (M_n) of the polymers. Because formation of macrocycles, having no end-groups, cannot be excluded, the values calculated may be to high [32,33].

The molecular weights (M_n) are denoted as > 50 kg mol^{-1} for the poly(ester amide)s with a hard segment content up to 56 mol%, due to the inaccuracy in the measurement of the integrals of the small signals corresponding to the end-groups. Poly(ester amide)s with a hard segment content of 78 and 85 mol% have a M_n of 39 and 20 kg mol^{-1}, respectively. These results show that the increasing deviation from the intended composition, by disturbing the stoichiometry, leads to a substantial decrease in M_n [27,34].

Previous work [35–37] has shown that a mixture of chloroform–methanol (1:1 vol/vol) is a suitable solvent for

Table 1
Chemical composition and physical properties of poly(ester amide)s with different hard segment content *x*

Polymer	Hard segment *x* (mol %)	M_n[a] (kg mol^{-1})	$[\eta]$[b] (dl g^{-1})	M_n[a,c] (kg mol^{-1})	$[\eta]$[b,c] (dl g^{-1})
PBA	0	27	0.43	27	0.39
PEA 90/10	10	>50	0.55	18	0.39
PEA 72/28	28	>50	0.59	20	0.52
PEA 44/56	56	>50	0.61	19	0.52
PEA 22/78	78	39	0.52	13	0.44
PEA 15/85	85	20	0.45	8	0.42

[a] According to ^{1}H NMR.
[b] $CHCl_3$/MeOH (1:1 vol/vol) at 25 °C.
[c] After compression moulding.

some kind of poly(ether ester amide)s. The intrinsic viscosity of the polymer (chloroform–methanol 1:1 vol/vol) was evaluated by capillary viscometry by extrapolation of the reduced ($\eta_{red}=\eta_{spec}c^{-1}$) and inherent ($\eta_{inh}=\ln(\eta_{rel})c^{-1}$) viscosities to $c=0$ [38]. A linear relationship was observed for PEA 72/28, suggesting that the chloroform–methanol mixture is a good solvent even at relatively high polymer concentrations. Extrapolating the reduced and inherent viscosities of PEA 72/28 to $c=0$ gives an intrinsic viscosity of 0.59 ± 0.01 dl g^{-1}. The intrinsic viscosity determined by a single point measurement at $c=\sim0.1$ g dl^{-1} is 0.59 dl g^{-1}, indicating that the single point measurement is representative for the intrinsic viscosity of PEA 72/28. Care should be taken when extrapolating these results to poly(ester amide)s with other compositions. In addition, since the Mark–Houwink constants are not known for the systems, the resulting intrinsic viscosities could not be converted to molecular weights.

The intrinsic viscosities of poly(ester amide)s before and after compression moulding are shown in Table 1. The synthesized poly(ester amide)s have intrinsic viscosities of 0.5–0.6 dl g^{-1}. The intrinsic viscosity decreased significantly upon compression moulding indicating that small amounts of absorbed moisture in poly(ester amide)s can already lead to hydrolytic chain scissions at elevated processing temperatures.

In Fig. 2, the FT-IR spectra of the PEA copolymers at room temperature are presented for the selected wave number regions, 3600–2700 and 1800–650 cm^{-1}. Characteristic IR-bands are found at 3305 (νN–H H-bonded), ~1730 (νC=O ester), 1634 (amide I, νC=O) and 1540 cm^{-1} (amide II, νC–N + δN–H). Several weaker IR-bands were observed at 1476, 1420 and 693 cm^{-1} belonging to the NH vicinal CH_2 bend, CO vicinal CH_2 bend and amide V,

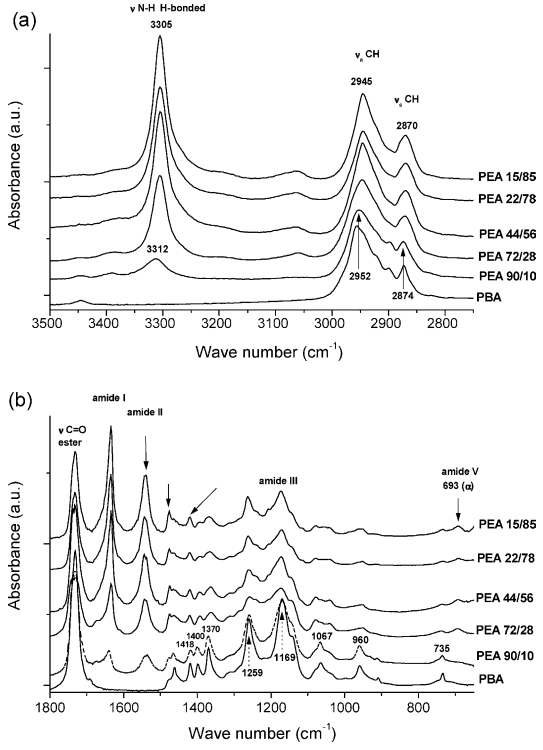

Fig. 2. (a) FT-IR spectra of PBA and PEA polymers with different hard segment content (10–85 mol%) at room temperature for the wave number region 3500–2700 cm^{-1}. (b) FT-IR spectra of PBA and PEA polymers with different hard segment content (10–85 mol%) at room temperature for the wave number region 1800–650 cm^{-1}.

In Fig. 2, the FT-IR spectra of the PEA copolymers at room temperature are presented for the selected wave number regions, 3600–2700 and 1800–650 cm^{-1}. Characteristic IR-bands are found at 3305 (νN–H H-bonded), ~1730 (νC=O ester), 1634 (amide I, νC=O) and 1540 cm^{-1} (amide II, νC–N + δN–H). Several weaker IR-bands were observed at 1476, 1420 and 693 cm^{-1} belonging to the NH vicinal CH_2 bend, CO vicinal CH_2 bend and amide V,

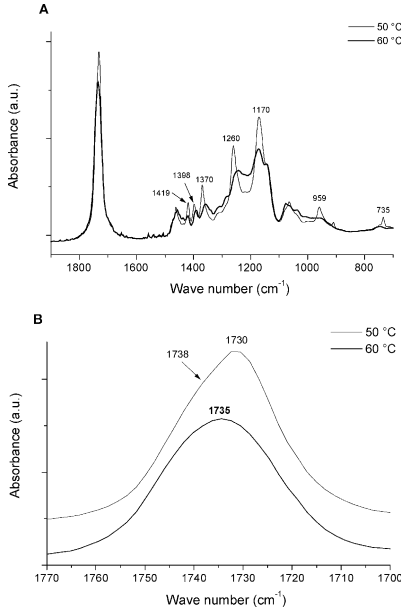

Fig. 3. FT-IR spectra of PBA at 50 and 60 °C for the wave number region 1900–700 cm^{-1}(A) and 1770–1700 cm^{-1}(B).

respectively. These latter IR-bands in combination with the amide II band provide important structural information. In polyamides like nylon 6,6 these bands are found at similar wave numbers, and are characteristic of a so-called α-crystalline phase. As only part of the structure of the bisamide-diol resembles the structure of nylon 6,6 the crystalline phase is denoted here as an α-type phase. Moreover, these bands are located at the same wave numbers as in the IR-spectra of the bisamide-diol monomer [29]. It thus seems that the α-type crystalline structure of the bisamide-diol is preserved in the poly(ester amide).

In a previous study, it was shown that only at a low amide content of ~10 mol% crystallization of butylene adipate segments takes place [14]. This is illustrated by the change in FT-IR spectra of poly(butylene adipate) (PBA) at elevated temperatures (Fig. 3). Upon heating PBA to the melt (60 °C), the IR-bands at 1419, 1398, 1370, 1260, 1170, 959 and 735 cm^{-1} (Fig. 3(A)), which are related to the crystalline part, disappear or decrease drastically in intensity. FT-IR spectra of PEA 90/10 also contain characteristic bands of crystalline PBA (Fig. 2(b)), which show that besides hard segments also polyester segments crystallize.

The carbonyl band of PBA at room temperature is highly asymmetric with a narrow top at 1730 cm^{-1} and a shoulder around 1738 cm^{-1} (Fig. 3(B)). Above 50 °C, the crystals melt and one broad band centred around 1735 cm^{-1} remains. This suggests that the absorption band at 1730 and 1738 cm^{-1} are associated with carbonyl groups in crystalline domains whereas the band at ~1735 cm^{-1} is associated with carbonyl groups in the amorphous phase [39]. However, care should be taken because curve fitting of this band is extremely difficult.

The band in the νC=O ester region of the PEA polymers consists of two bands at ~1730 and ~1738 cm^{-1} (Fig. 4). Since the soft polyester segments crystallize only in poly(ester amide)s with a hard segment content ≤10 mol%, these results suggest that ester sequences in the hard segment of poly(ester amide)s with higher (>10 mol%) hard segment content are incorporated in the crystals.

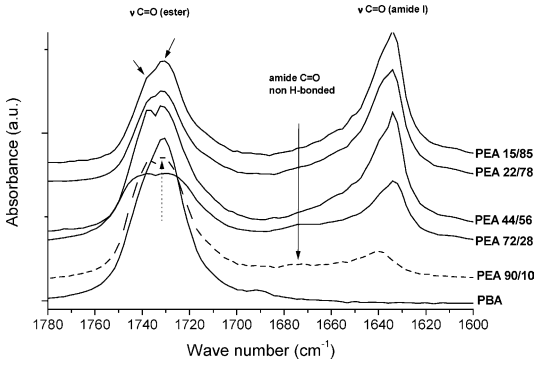

Fig. 4. FT-IR spectra of PBA and PEA polymers with different hard segment content (10–85 mol%) at room temperature for the wave number region 1780–1600 cm^{-1}.

The WAXD spectra (Fig. 5) of the PEA polymers show typical reflections of an α-type crystalline phase similar to the well-defined α-crystalline phase in nylon 6,6. These reflections represent the distance between two amide–amide intermolecular H-bonded chains (~4.8 Å) and the distance between two van der Waals packed sheets (3.7 Å). In the WAXD spectra of the poly(ester amide)s the *d*-spacing (4.34–4.41 Å) representing the distance between two amide–amide intermolecular H-bonded chains is found at a somewhat lower value as found for the *d*-spacing as of nylon 6,6. The differences observed may be result of the incorporation of ester units in the crystalline structure. The distance between the two van der Waals packed sheets (3.98–3.87 Å) in the poly(ester amide)s is somewhat larger than in nylon 6,6. The comparable values of the *d*-spacing in the PEA polymers and nylon 6,6 and the structural data obtained from FT-IR lead to the assumption that the chains are in the fully extended planar zig-zag conformation forming H-bonded planar sheets typical for an α-crystalline phase. Note that a typical reflection of an γ-type crystalline phase (4.12 Å) is present for PEA 72/28.

3.2. Thermal properties

The thermal stability of the segmented poly(ester amide)s under non-oxidative conditions was investigated by thermal gravimetric analysis (TGA). PBA is stable up to 380 °C and segmented poly(ester amide)s are stable up to ~340 °C. For all polymers the decomposition temperatures are considerably higher than the melting temperature, which is important for the processing of these materials.

The crystallization and melting temperatures and corresponding enthalpies of the poly(ester amide)s were taken from the first cooling and second heating scan as measured by DSC (Table 2). All PEA polymers show two melt transitions denoted as $T_{m,1}$ and $T_{m,2}$ for the low and high melt transition, respectively.

Upon cooling from the melt, the poly(ester amide)s show a complex crystallization pattern with one or even multimodal transitions depending on the hard segment content

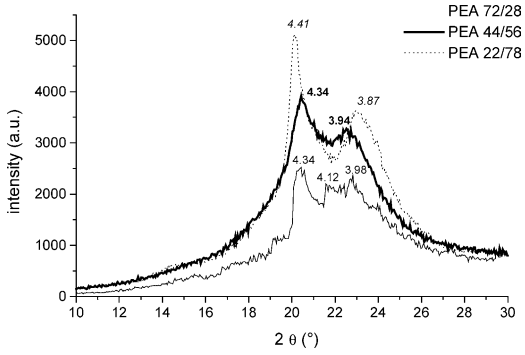

Fig. 5. WAXD spectra of PEA 72/28, PEA 44/56 and PEA 22/78 at room temperature. Polymers were heated to the melt, annealed for 10 min and subsequently cooled to 30 °C at 20 °C min^{-1}. The data represent the *d*-spacings in Å.

(Fig. 6). Only in the poly(ester amide) with a high ester content (PEA 90/10) crystallization of PBA is possible. However, the corresponding exotherm at −7 °C, is found at a somewhat lower temperature compared to that of the homopolymer PBA (24 °C). The exotherm at 22 °C is due to the presence of crystals comprising EA segments.

Statistically, at low hard segment content, the number average ester amide (EA) sequence length k increases from 1.1 for PEA 90/10 to 1.4 for PEA 72/28 [28,40]. This value is approximately 2.2 for PEA 44/56 and 4.2 for the PEA 22/78. This suggests that the crystalline phase at low amide content constitutes single EA sequences whereas the crystalline phase at high amide content contains two or more EA sequences. Moreover, in the IR-spectra of PEA polymers ($x > 10$ mol%) a band was found at 1730 cm^{-1} corresponding with ester carbonyl groups in the crystalline phase, which confirms the formation of crystals comprising two or more EA sequences.

During cooling, a multi-modal exotherm was observed in the DSC scan of PEA 44/56 which might be due to the presence of a mixture of crystals with different EA sequence lengths. At high EA content the T_c eventually shifts to temperatures of 111 °C, but also a small transition still can be observed at ~30 °C due to a crystalline phase containing single EA sequences.

Upon reheating, the poly(ester amide)s show an endothermic transition ($T_{m,1}$) between 58 and 70 °C followed by a second transition ($T_{m,2}$) (Fig. 7). PEA 90/10 shows a broad melt transition at 59 °C, which is attributed to melting of crystalline PBA segments and of crystals that consist of single EA sequences. PEA 72/28 shows an exotherm directly after the first melt transition, at which probably crystals are rearranged into a more stable crystalline structure.

The first melting temperature was almost independent of the polymer hard segment content (Fig. 8). However, the corresponding melt enthalpies decreased with increasing hard segment (Fig. 9). The higher probability of having crystals consisting of more successive EA sequences at higher hard segment content explains the decreasing melt enthalpy ($\Delta H_{m,1}$) [28]. The second melting temperature ($T_{m,2}$), at which crystals comprising two or more EA sequences melt, increases with decreasing soft segment

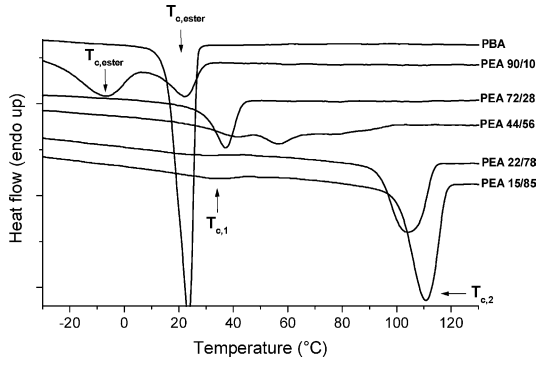

Fig. 6. DSC cooling scans (20 °C min^{-1}) of PBA and PEA polymers with different hard segment content (10–85 mol%).

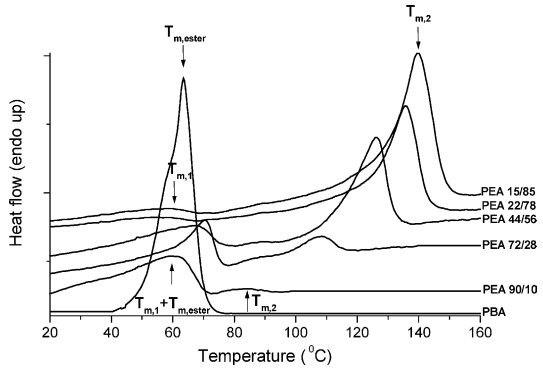

Fig. 7. DSC heating scans (20 °C min^{-1}) of PBA and PEA polymers with different hard segment content x (10–85 mol%).

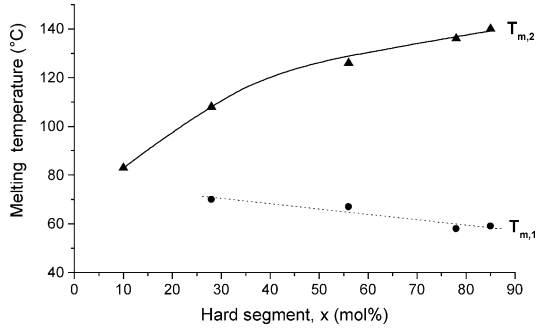

Fig. 8. Low ($T_{m,1}$) and high ($T_{m,2}$) melting temperatures of PEA polymers as a function of hard segment content x.

Table 2
Thermal properties of PEA polymers with different hard segment content x (10–85 mol%)

Polymer	$T_{m,1}$ (°C)	$\Delta H_{m,1}$ (J g^{-1})	$T_{c,1}$ (°C)	$\Delta H_{c,1}$ (J g^{-1})	$T_{m,2}$ (°C)	$\Delta H_{m,2}$ (J g^{-1})	$T_{c,2}$ (°C)	$\Delta H_{c,2}$ (J g^{-1})
PBA					63	58	24	−57
PEA 90/10	59[a]	35	–	–	83	1	−7, 22[b]	−39
PEA 72/28	70	24	–	–	108	9	37	−23
PEA 44/56	67	16	–	–	126	32	54, 56, 79[c]	−34
PEA 22/78	58	4	22	−4	136	45	104	−42
PEA 15/85	59	4	32	−4	140	58	111	−47

[a] $T_{m,1} + T_{m,ester}$.
[b] Two peaks.
[c] Trimodal.

content. This is a general trend observed for segmented copolymers and is explained by the solvent effect proposed by Flory [41]. Upon dilution of the crystallizable hard segment thus increasing the molar fraction of soft segment, the size of the crystals will become smaller and hence its melting temperature decreases. Also with increasing hard segment content the average length of the hard segment and thus the crystal lamellar size increases, resulting in a higher melting temperature [42]. Probably, the increasing melting temperature with increasing hard segment content is a consequence of both effects although $T_{m,2}$ is levelling off at higher hard segment contents to ~140 °C. The corresponding enthalpies still increase with increasing hard segment content.

The crystallinity of the poly(ester amide)s, calculated by deconvolution of the IR-band of the amide I, increased with increasing hard segment content (Table 3).

3.3. Dynamic mechanical properties

Similar to $T_{m,2}$, the flow temperature as obtained from DMA measurements increased with increasing hard segment content (Table 3). This transition is very sharp for all poly(ester amide)s.

Poly(ester amide)s with a hard segment content > 25 mol% show a transition in the rubber plateau (Fig. 10). This transition is found at temperatures corresponding with the lower melting temperature ($T_{m,1}$) obtained from DSC measurements.

DSC traces only showed weak transitions at the polymer T_g, which made their evaluation rather imprecise. For this reason, only T_g data obtained from DMA measurements are reported here. The T_g of the poly(ester amide)s is linearly increasing with increasing hard segment content (Table 3) [14]. This suggests that the phase separation is not complete and that hard segments are molecularly dispersed throughout the amorphous soft phase forming a homogeneous amorphous phase [40].

The storage modulus at 25 °C, which is a measure for the crystallinity, increased with increasing hard segment content x (Table 3). This increase is due to an increased physical crosslink density at higher hard segment content.

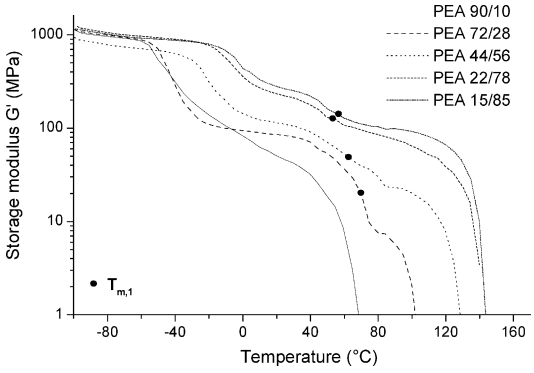

Fig. 10. Storage modulus as a function of temperature for PEA polymers with different hard segment content x (10–85 mol%).

3.4. Mechanical properties

Typical stress–strain curves for the segmented poly(ester amide)s are presented in Fig. 11. The E modulus is determined at small deformations (0.1%) where stress increases linearly with strain (Hooke's law). At the yield point, necking occurs and the plateau in the stress–strain curve reflects the growing of the neck. Finally, the stress level becomes high enough to cause chain breakage and sample failure. Such a deformation process is well known for segmented copolymers [43,44].

The PEA polymers with a high hard segment content display a stress–strain curve typical of glassy or crystalline homopolymers with a pronounced yield point followed by break at relatively low strains.

By increasing the hard segment content from 10 to 85 mol%, the E modulus increases from 70 to 524 MPa, the yield stress increases from 9 to 22 MPa while the strain at break decreases from 820 to 370% (Table 4). The homopolymer PBA has a high E modulus and tensile strength but is very brittle. By the incorporation of bisamide-diol moieties into the backbone of PBA the elastic modulus, yield stress and stress at break remained high but

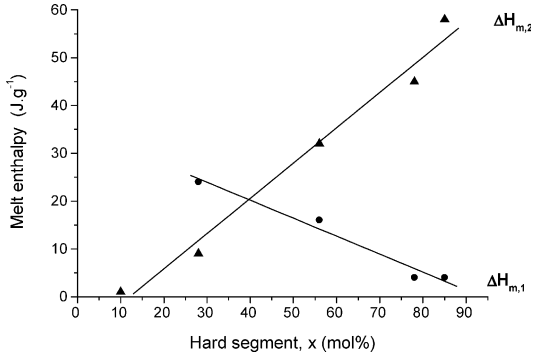

Fig. 9. Melting enthalpies $\Delta H_{m,1}$ and $\Delta H_{m,2}$ for the low and high T_m transitions of PEA polymers as a function of hard segment content x.

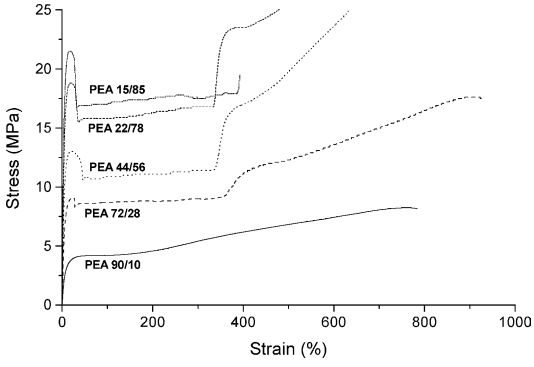

Fig. 11. Stress strain curves for injection moulded samples of PEA polymers with different hard segment content x (10–85 mol%).

Table 3
Thermal properties of PEA polymers with different hard segment content x, as obtained from DMA and DSC

Polymer	Hard segment x (mol %)	T_{flow}[a] (°C)	$T_{m,2}$[b] (°C)	w_c[c] (mol%)	$G'_{25\,°C}$ (MPa)	T_g[a] (°C)
PBA		60	63		140	−52
PEA 90/10	10	70	83	5±2.5	34	−45
PEA 72/28	28	105	108	12.5±2.5	62	−40
PEA 44/56	56	130	126	27.5±2.5	103	−20
PEA 22/78	78	146	136	42.5±2.5	203	−8
PEA 15/85	85	145	140	42.5±2.5	274	−5

[a] From DMA.
[b] From DSC.
[c] Crystallinity according to amide I band in FT-IR spectra.

the strain at break increased to a large extent. Thus these poly(ester amide)s are tough materials with a high stiffness. The mechanical properties of these segmented poly(ester amide)s are similar to low density polyethylene ($T_g \sim -25$ °C, $T_m = 98$–115 °C), which has an elastic modulus in the range of 170–280 MPa, a stress at break in the range of 8–30 MPa and a strain at break in the range of 100 to 650%. The mechanical properties also correspond well with segmented poly(ester amide)s based on 1,6-diaminohexane, γ-butyrolactone, 1,2-ethanediol and dimethyl adipate which revealed an elastic modulus up to 600 MPa and a yield stress up to 10 MPa with increasing hard segment content [18].

Polymer samples were processed by compression as well as injection moulding in order to determine the influence of these processing steps on the mechanical properties (Table 4). Overall, the mechanical properties of both series of polymer are comparable. In general, injection moulded samples have a lower crystallinity compared to compression moulded samples because the latter is cooled down at lower rate. This is reflected in the somewhat higher modulus and yield stress for the compression-moulded samples. The strain at break for the compression moulded film of PEA 15/85 is significantly lower compared to that of the injection moulded film, which might be due to their low molecular weight.

Complete elastic recovery is hardly observed for thermoplastic elastomers (TPE's) [20]. During deformation polymer chains in a network held together by entanglements and other physical interactions are stretched. Above the yield point reorganization takes place, the crystalline network as well as the crystalline lamellae start to disrupt. After release of the external stress the polymer chains retract to their original position with a gain in entropy as the driving force for the recovery. However, only part of the material recovers. The non-recoverable plastic deformation is due to permanent viscous flow of the polymer chains. Relaxation in semi-crystalline polymers is associated with the amorphous component, the crystalline component or an interaction whereby the crystalline component constrains the motion of the amorphous phase [42,46]. In TPE's the soft segments usually relax to the non-oriented state while the hard domains remain oriented which leads to a considerable amount of permanent set [42,45]. Long soft segments are less influenced by the restricting behaviour of the hard domains and will accordingly be better capable of accommodating deformation without breaking and will retract more readily, resisting set. In general, a higher hard segment content leads to a higher permanent set in segmented copolymers [46,47].

To measure the compression set (CS) at room temperature, polymer bars are compressed to 75% of their original thickness and thus the polymers are strained above their yield point (Table 5). During the compression test the polymer is deformed to some state of strain (25% of compression) and secured in such a way that it retains the initial deformation. Since the material behaves visco-elastic, the stress level is lowered (relaxation) during the experiment (in time). After release of the external stress, the polymer system will show a time-dependent strain

Table 4
Mechanical properties of PBA and PEA polymers with different hard segment content

Polymer	E modulus (MPa)		Yield stress (MPa)		Stress at break (MPa)		Strain at break (%)	
	com[a]	inj[b]	com[a]	inj[b]	com[a]	inj[b]	com[a]	inj[b]
PBA	415±24	477±20	15±0.5	–	15±0.5	17±1.5	150±20	10±5
PEA 90/10	73±6	70±11	4±0.5	–	8±0.5	8±0.5	870±35	820±45
PEA 72/28	180±36	180±35	9±0.5	9±0.5	15±1	16±1	810±100	840±60
PEA 44/56	270±42	274±30	14±0.5	13±0.5	25±1	26±0.5	680±30	660±10
PEA 22/78	473±27	432±36	23±1	18±1	24±1.5	28±2	420±20	580±25
PEA 15/85	553±47	524±59	26±1	22±1	25±2	22±1	50±15	370±25

[a] Compression moulded bars.
[b] Injection moulded bars.

Table 5
Compression set of injection moulded samples of PEA polymers with different hard segment content x (10–85 mol%)

Polymer	Hard segment x (mol %)	$\sigma_{at\ yield}$ (MPa)	$\varepsilon_{at\ yield}$ (%)	$CS_{25\%}$ (%)
PEA 90/10	10	–	–[a]	35±2
PEA 72/28	28	9±0.5	24±2	39±5
PEA 44/56	56	13±0.5	18±2	49±6
PEA 22/78	78	18±1	16±1	30±5
PEA 15/85	85	22±1	16±0.5	5±2

[a] No yield point.

relaxation. The compression set of the PEA polymers increases with increasing hard segment content up to 56 mol%. Surprisingly, the compression set starts to decrease by increasing the hard segment content to 85 mol%. However, PEA polymers with a high hard segment content have a higher stiffness (higher modulus and yield stress) compared to PEA polymers with a low hard segment content (Table 4) and thus the initial force (stress) to sustain a similar deformation will be higher. It is thus understandable that PEA polymers with a high hard segment content respond differently with respect to relaxation (elastic recovery) as compared to PEA polymers with a low hard segment. In addition, the elastic recovery is time dependent and relaxation time in our experiment (30 min) is probably not enough to reach a state of equilibrium.

3.5. Water uptake

The polymer water absorption was determined by placing polymer samples in a dessicator at room temperature at 100% relative humidity (RH) or immersing polymer samples in water at 37 °C. The water absorption of poly(ester amide) samples was followed in time over a period of 3 weeks. Polymers show an increase in water absorption in time, which is levelling off at prolonged times (equilibrium). PBA shows a low water absorption of 0.7% at equilibrium. Polyamides are known to have high water absorption [48], and it was expected that with increasing bisamide content the water absorption will increase.

Water absorption of polymers at 100% RH, is maximal at a hard segment content of ~50 mol% (Table 6). The polymers PEA 22/78 and PEA 15/85 show a lower water absorption than expected based on their amide content, which can be ascribed to the higher crystallinity of these materials. The polymers immersed in water at 37 °C show a decreasing water absorption with increasing hard segment content. Apparently the increasing crystallinity is more important than the increasing amide content. The very high water uptake of PEA 90/10 is probably caused by partial melting of the polymer at 37 °C (Fig. 7), which decreases the crystallinity.

4. Conclusions

High molecular weight segmented poly(ester amide)s comprising different ester to amide ratios have been successfully prepared by melt polycondensation of a preformed bisamide-diol, 1,4-butanediol and dimethyl adipate. The polymers have melt transitions between 58 and 70 °C and between 83 and 140 °C, depending on the hard segment content, and a sub-ambient glass transition temperature (−45 to −5 °C). The poly(ester amide)s have a micro-phase separated structure with an amide-rich hard phase and an ester-rich flexible soft phase. The poly(ester amide)s crystallize in an α-type phase similar to even–even nylons. The presence of α-related bands in the IR- and WAXD-spectra of the bisamide-diol monomer indicates that the α-type crystalline structure of the bisamide-diol is preserved in the poly(ester amide).

By increasing the hard segment content from 10 to 85 mol% the elastic modulus increased from 70 to 524 MPa, the stress at break increased from 8 to 28 MPa while the strain at break decreased from 820 to 370%. It can be concluded that the incorporation of well-defined amide segments in the poly(butylene adipate) backbone results in improved thermal and mechanical properties compared to the homopolymer poly(butylene adipate). Furthermore, these properties can be tuned for specific applications by varying the hard segment content in these segmented polymers.

Table 6
Equilibrium water uptake of PBA and PEA polymers with different hard segment content, conditioned at 100% relative humidity at room temperature or immersed in water at 37 °C

Polymer	Time[a] (days)	Water uptake (%)	Time[b] (days)	Water uptake (%)
PBA	3	0.7	1	1.0±0.2
PEA 90/10	6	3.8	5[c]	14.7±0.2
PEA 72/28	6	5.7	3	11.7±0.1
PEA 44/56	6	7.5	2	9.4±0.1
PEA 22/78	6	6.1	5	8.8±0.1
PEA 15/85	6	5.9	3	7.8±0.2

[a] Time to reach equilibrium at RH = 100%.
[b] Time to reach equilibrium after immersion in water at 37 °C.
[c] Not at equilibrium.

Acknowledgements

The authors thank Herman Koster for the WAXD measurements. This study was financially supported by the European Commission, project: QLK5-1999-01298.

References

[1] Grigat E, Koch R, Timmermann R. Polym Degrad Stab 1998;59(1–3):223–6.
[2] Ferré T, Franco L, Rodríguez-Galán A, Puiggalí J. Polymer 2003;44:6139–52.
[3] Wiegand S, Steffen M, Steger R, Koch R. J Environ Polym Degrad 1999;7(3):145–55.
[4] Gonsalves KE, Chen X, Cameron JA. Macromolecules 1992;25:3309–12.
[5] Lee SY, Park JW, Yoo YT, Im SS. Polym Degrad Stab 2002;78:63–71.
[6] Qian ZY, Li S, He Y, Li C, Liu X. Polym Degrad Stab 2003;81:279–86.
[7] Qian ZY, Sai L, Hailian Z, Xiaobo L. Colloid Polym Sci 2003;281:869–75.
[8] Alla A, Rodríguez-Galán A, Martínez de llarduya A, Muñoz-Guerra S. Polymer 1997;38(19):4935–44.
[9] Pérez-Rodríguez A, Alla A, Fernández-Santín JM, Muñoz-Guerra S. J Appl Polym Sci 2000;78:486–94.
[10] Andini S, Ferrara L, Maglio G, Palumbo R. Macromol Chem Rapid Commun 1988;9:119–24.
[11] Castaldo L, de Candia F, Maglio G, Palumbo R, Strazza G. J Appl Polym Sci 1982;27:1809–22.
[12] Armelin E, Paracuellos N, Rodríguez-Galán A, Puiggalí J. Polymer 2001;42:7923–32.
[13] Kawasaki N, Nakayama A, Maeda Y, Hayashi K, Yamamoto N, Aiba S. Macromol Chem Phys 1998;199:2445–51.
[14] Stapert HR, Dijkstra PJ, Feijen J. Macromol Symp 1998;130:91–102.
[15] Stapert HR, Dijkstra PJ, Feijen J. Macromol Symp 2000;152:127–37.
[16] Pivsa-Art S, Nakayama A, Kawasaki N, Yamamoto N, Aiba S. J Appl Polym Sci 2002;85(4):774–84.
[17] Castaldo L, Maglio G, Palumbo R. Polym Bull 1992;28:301–7.
[18] Bera S, Jedlinski Z. Polymer 1992;33(20):4331–6.
[19] Bera S, Jedlinski Z. J Polym Sci, Part A: Polym Chem 1993;31(3):731–9.
[20] Holden G, Legge NR, Quirk R, Schroeder HE. Thermoplastic elastomers. New York: Hanser; 1996.
[21] Miller JA, Lin SB, Kirk KS, Hwang KS, Wu KS, Gibson PE, et al. Macromolecules 1985;18(1):32–44.
[22] Gaymans RJ, de Haan JL. Polymer 1993;34(20):4360–4.
[23] Ng HN, Allegrezza AE, Seymour RW, Cooper SL. Polymer 1973;14:255–61.
[24] Harrell LL. Macromolecules 1969;2(6):607–12.
[25] Kaczmarczyk B. Polymer 1998;39(23):5853–60.
[26] Kaczmarczyk B, Sek D. Polymer 1995;36(26):5019–25.
[27] Stapert HR, Bouwens AM, Dijkstra PJ, Feijen J. Macromol Chem Phys 1999;200(8):1921–9.
[28] Stapert HR. PhD Thesis. The Netherlands: University of Twente; 1998. p. 121.
[29] Lips PAM, van Heeringen MJM, Broos R, Dijkstra PJ, Feijen J. Submitted for publication.
[30] Solomon OF, Ciuta IZ. J Appl Polym Sci 1962;6:683–6.
[31] Shroff RN. J Appl Polym Sci 1965;9:1547–51.
[32] Kricheldorf HR, Rabenstein M, Maskos M, Schidt M. Macromolecules 2001;34:713–22.
[33] Kricheldorf HR, Böhme S, Schwarz G. Macromolecules 2001;34:8879–85.
[34] Pilati F, Manaresi B, Fortunato B, Munari A, Monari P. Polymer 1983;24:1479–83.
[35] Deschamps AA, Grijpma DW, Feijen J. J Biomater Sci Polym Ed 2002;13(12):1337–52.
[36] Signori F, Solaro R, Chiellini E, Lips PAM, Dijkstra PJ, Feijen J. Macromol Chem Phys 2003;204(16):1971–81.
[37] Signori F, Solaro R, Lips PAM, Dijkstra PJ, Feijen J, Chiellini E. Macromol Chem Phys 2004;204(16):1299–308.
[38] Billmeyer FW. Structure and properties of polymers. Textbook of polymer science. New York: Wiley-Interscience; 1962.
[39] Fei B, Chen C, Wu H, Peng S, Wang X, Dong L. Eur Polym J 2003;39:1939–46.
[40] Cella RJ. J Polym Sci 1973;42:727–40.
[41] Flory PJ. J Chem Soc Faraday Trans 1955;51:848–57.
[42] Sperling LH. Introduction to physical polymer science. New York: Wiley-Interscience; 2001.
[43] Niesten MCEJ, Harkema S, van der Heide E, Gaymans RJ. Polymer 2001;42:1131–42.
[44] Bonart R. J Macromol Sci Phys 1968;B2(1):115–38.
[45] McCrum NG, Buckley CP, Bucknall CB. Principles of polymer engineering. Oxford: Oxford University Press; 1991.
[46] Niesten MCEJ, Gaymans RJ. J Appl Polym Sci 2001;81:1372–81.
[47] Krijgsman J, Husken D, Gaymans RJ. Polymer 2003;44:7573–88.
[48] Kohan MI. Nylon plastic handbook. New York: Hanser; 1995.